

Connection between hysteresis, Barkhausen noise, and microstructure in magnetic materials

G. Durin,^{a)} C. Beatrice, C. Appino, V. Basso, and G. Bertotti

Istituto Elettrotecnico Nazionale Galileo Ferraris and INFM, Corso M. d'Azeglio 42, I-10125 Torino, Italy

The interplay between material microstructure and magnetic hysteresis is studied in rapidly quenched Si-Fe alloys. Two ribbons of different average grain dimension $\langle s \rangle$ (35 and 160 μm) were prepared by annealing at different temperatures and studied through two independent approaches: Barkhausen noise measurements, and Preisach analysis of static and dynamic hysteresis loops. In order to monitor the effect of demagnetizing fields on the magnetization process, the strips were progressively shortened from 30 to 10 cm. The correlation length of a domain-wall jump was estimated through the analysis of Barkhausen jump distributions versus apparent permeability. The correlation length of the coherent magnetization reversals controlling excess dynamic losses was estimated through the Preisach analysis of dynamic hysteresis loops. In the sample with lower $\langle s \rangle$, both the Barkhausen and the dynamic loss correlation lengths are comparable to $\langle s \rangle$, showing that a single structural feature governs all aspects of magnetization reversal. Conversely, in the high $\langle s \rangle$ sample, the ribbon thickness competes with $\langle s \rangle$ in controlling static and dynamic magnetization processes. © 2000 American Institute of Physics. [S0021-8979(00)77808-X]

I. INTRODUCTION

The connection between magnetic hysteresis and microstructure has been extensively investigated in the past. The major difficulty is always the identification of a few relevant parameters summarizing the role of the microstructure in an adequate way. In soft polycrystalline materials, the average grain dimension has been shown to control coercivity and excess dynamic losses under several circumstances,^{1,2} but it is not clear how general this connection can be and how it might be generalized to amorphous and nanocrystalline systems, where other characteristic lengths are expected to play the role of effective grain size, such as, for example, the wavelength of quenched-in stress fluctuations.³ In addition, also the geometrical parameters, like the thickness in thin ribbons, might play a significant role under particular conditions. These difficulties indicate that a more detailed analysis of microscopic magnetization mechanisms is needed, in order to achieve some general conclusions about microstructure-controlled magnetic properties.

In this respect, a key role is played by the Barkhausen effect. The signal measured in a Barkhausen experiment reflects the details of magnetization reversal mechanisms and in principle contains rich information about microstructure-controlled processes. In particular, one can exploit recent Barkhausen-effect models^{4,5} to estimate the typical correlation length involved in single magnetization reversal events. This length is controlled by the microstructure and by demagnetizing counterfields, which tend to fragment reversal events into smaller jumps. Through Barkhausen-effect measurements under different demagnetizing fields, one can estimate the correlation length upper limit under vanishing de-

magnetizing effects, which is expected to be controlled by the microstructure only. Interestingly, a magnetization reversal correlation length is also involved in the processes responsible for excess dynamic losses. As previously mentioned, in polycrystalline materials, this correlation length is often found to be close to the grain size,² but its general connection to the microstructure is still poorly understood. For example, it is not clear if, similarly to the Barkhausen-effect case, also this correlation length should be affected by demagnetizing effects, and if these two lengths should eventually match.

The purpose of this article is to investigate these issues in rapidly quenched 6.5 wt % Si-Fe nonoriented polycrystalline materials, by measurements of hysteresis and loss properties, combined with Barkhausen-effect experiments, in ribbons of variable length and variable grain size.

II. EXPERIMENTAL METHODS AND DATA ANALYSIS

Various rapidly quenched 6.5 wt % Si-Fe ribbons (width=10 mm, thickness $\cong 45 \mu\text{m}$) were prepared by the planar-flow-casting technique. Two ribbons with different average grain size [$\langle s \rangle = 35 \mu\text{m}$ (sample A) and $\langle s \rangle = 160 \mu\text{m}$ (sample B)] were obtained by annealing the as-cast material for 2 h at 1050 and at 1200 °C, respectively. In order to monitor the effect of demagnetizing fields on the magnetization process, measurements were carried out on ribbons progressively shortened from 30 to 10 cm, changing the apparent permeability μ_{app} over one order of magnitude. For each length, the following measurements were carried out: (i) a set of static symmetric minor loops with different peak inductions up to 1.2 T, to reconstruct the Preisach distribution;⁶ (ii) a set of dynamic hysteresis loops at 0.5 and 1 T, measured under controlled sinusoidal induction at several magnetization frequencies in the range 1 Hz–10 kHz, to

^{a)}Electronic mail: durin@omega.ien.it

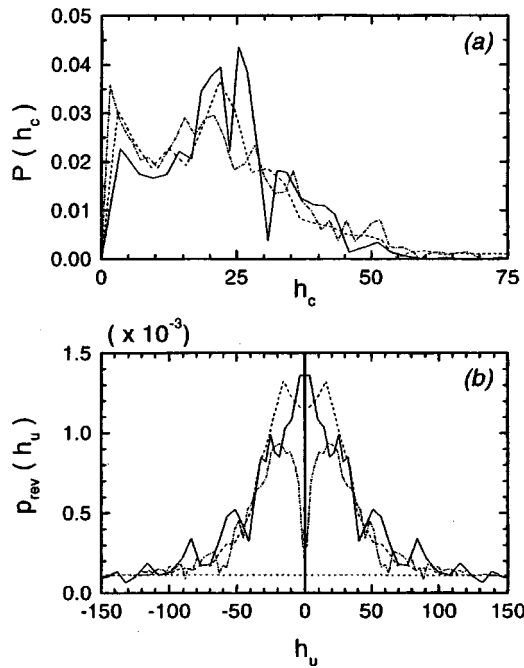


FIG. 1. Distribution of local pinning fields; $P(h_c) = \int p_{irr}(h_c, h_u) dh_u$ (a), and reversible component, $p_{rev}(h_u)$ (b), of the Preisach distribution $p(h_c, h_u) = p_{irr}(h_c, h_u) + \delta(h_c) p_{rev}(h_u)$ for sample B ($\langle s \rangle = 160 \mu\text{m}$) at three different ribbon lengths L ($L = 10$ cm: solid lines; $L = 20$ cm: dashed lines; $L = 28.3$ cm: dash-dot lines).

estimate the dynamic loss correlation length;⁷ and (iii) Barkhausen-effect signal, measured in the central part of the 1 T hysteresis loop under a triangular applied field wave form, at magnetization rates in the range $0.1\text{--}0.6 \text{ T s}^{-1}$, to determine the signal amplitude distribution, and the probability distribution of Barkhausen jump duration and size.^{4,8}

From the set of static symmetric minor loops, one can reconstruct the Preisach distribution, according to the method discussed in Ref. 6. The use of symmetric loops is equivalent to that of first-order return branches often discussed in the literature,⁹ with the advantage of forcing the reconstructed distribution $p(h_c, h_u)$ to have the correct symmetry $p(h_c, h_u) = p(h_c, -h_u)$. The method yields two pieces of information: the shape of the Preisach distribution $p(h_c, h_u)$ and the behavior of the mean-field constant k_m controlling the relationship between the applied field H_a and the effective field H acting in the Preisach plane, $H = H_a + k_m I$, where I is the magnetization. Similarly to other cases studied in the literature,⁶ the distribution $p(h_c, h_u)$ appears to be the combination of a two-dimensional component $p_{irr}(h_c, h_u)$ in the $h_c > 0$ half-plane, associated with irreversible magnetization processes, and of a one-dimensional component $p_{rev}(h_u)$ along the $h_c = 0$ axis, describing reversible mechanisms. The behavior of p_{irr} is conveniently summarized by considering its integral with respect to h_u , $P(h_c)$, which can be approximately interpreted as the distribution of local pinning fields in the material. Figure 1 shows the functions $P(h_c)$ and $p_{rev}(h_u)$ obtained for sample B, at three different ribbon lengths. Similar results were found for sample A. Within the errors of the estimation, the Preisach distribution is independent of the apparent permeability.

The behavior of mean-field effects is shown in Fig. 2,

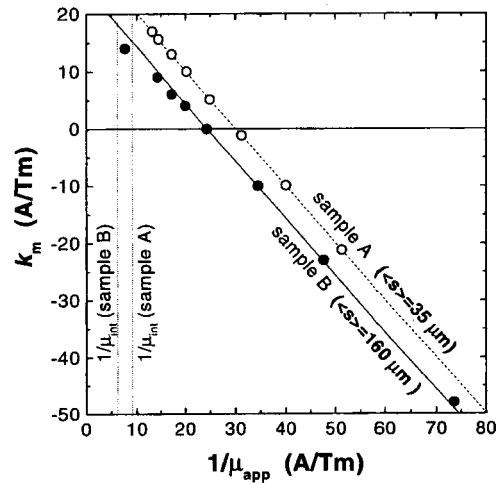


FIG. 2. Mean-field constant k_m of the effective field acting in the Preisach plane ($H = H_a + k_m I$), as a function of the apparent permeability for samples A ($\langle s \rangle = 35 \mu\text{m}$) and B ($\langle s \rangle = 160 \mu\text{m}$).

where k_m is plotted as a function of the inverse of the apparent differential permeability μ_{app} measured around coercivity at different ribbon lengths. If demagnetizing fields were the only mechanism contributing to k_m , one would expect $k_m = -(1/\mu_{app} - 1/\mu_{int})$, where μ_{int} is the intrinsic permeability of a ribbon of infinite length. An attempt to estimate μ_{int} was made by measuring the hysteresis loop in a closed magnetic circuit configuration, where flux closure was provided by a permalloy yoke. This gave $\mu_{yoke} \cong 0.11$ (sample A), and $\mu_{yoke} \cong 0.16 \text{ Tm/A}$ (sample B). One would expect $k_m \cong 0$ when $\mu_{app} \cong \mu_{yoke}$, but Fig. 2 shows that is definitely not the case. The dependence of k_m on μ_{app} is better described by the law $k_m = k_0 - (1/\mu_{app} - 1/\mu_{int})$, where the parameter k_0 summarizes the internal mean-field mechanisms active in the material, due to microstructure-controlled magnetostatic and/or exchange interactions. By assuming $\mu_{int} = \mu_{yoke}$, we found values quite similar in the two samples: $(k_0)_A \cong 21 \text{ A T}^{-1} \text{ m}^{-1}$, and $(k_0)_B \cong 18.5 \text{ A T}^{-1} \text{ m}^{-1}$. Interestingly, the internal and the geometrical mean-field effects simply sum up. Therefore, in principle, one could adjust the demagnetizing contribution in a way to balance out the internal one and to obtain a situation of negligible total mean-field contribution.

The static Preisach analysis cannot give any information about spatial correlation effects. In other words, one obtains local coercive field distributions, as in Fig. 1(a), but no information about the typical size of the magnetization reversal events associated with these fields. Such information is obtained considering the dynamic Preisach model.⁷ This model predicts the dependence of dynamic hysteresis loop shapes on the basis of the static Preisach distribution and of the average size of the correlation regions where the magnetization coherently reverses under dynamic conditions. Fitting of measured dynamic loops gives the number N_0 of these correlation regions in the ribbon cross section and the associated correlation length $\delta_c = \sqrt{A/N_0}$, where A is the ribbon cross-sectional area. The length δ_c is found to be independent of demagnetizing effects in both samples (Fig. 3).

The Barkhausen effect can bring information about the correlation length of individual magnetization reversal

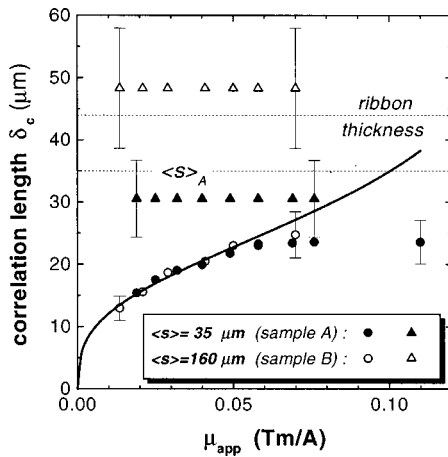


FIG. 3. Comparison of the correlation length δ_c estimated from Barkhausen effect (dots) and dynamic Preisach model (triangles). The solid line represents the behavior expected when only the variation of the demagnetizing factor is taken into account [see Eq. (2)].

events occurring along the static hysteresis loops. At low-magnetization rates, various sources of disorder make the domain-wall motion highly irregular, which results in a series of random Barkhausen jumps. As extensively reported,¹⁰ the probability distributions of jump duration and size follow power laws with well-defined critical exponents.^{4,8} In particular, the jump size S follows a law of the type

$$P(S) \sim S^{-\tau} f(S/S_0), \quad (1)$$

where S_0 is the cutoff size, i.e., the largest flux change produced by a wall jump. The critical exponent τ has been shown to be universal, i.e., independent of the details of the magnetic structure and given only by the range of interactions acting on the wall and by the dimensionality of the system. For instance, the measurements reported in Ref. 5 show that $\tau \approx 1.5$ in many polycrystalline Si-Fe ribbons with different microstructure. Conversely, the cutoff size S_0 is expected to depend on the microstructure of the material, and on the demagnetizing counterfield. The effect of a varying demagnetizing factor can be theoretically predicted, as shown in detail in Ref. 5. Here, we summarize the conclusions relevant to the interpretation of the present experiments. The analysis is based on an equation of domain-wall motion where the mean-field geometrical effects given by the demagnetizing field $H_{\text{dem}} = -kI$ are summed up with fine-scale random effects, due to dipolar interactions and structural disorder. Remarkably, this is in agreement with the results of the Preisach analysis previously discussed, where the mean-field parameter k_m was expressed as the sum of the demagnetizing factor and an internal mean-field parameter k_0 summarizing the role of the different interactions. Assuming that the structural disorder of the system could be described by a Gaussian-distributed white process of amplitude of fluctuations D , S_0 is predicted to scale as $S_0 \sim D(k/J_0)^{-2/3}$, where J_0 measures the strength of dipolar interactions.

We will define the Barkhausen correlation length as $\delta_c = \sqrt{S_0/2I_s}$. In terms of δ_c , the scaling relation $S_0 \sim k^{-2/3}$ becomes

$$\delta_c \sim \left(\frac{1}{\mu_{\text{app}}} - \frac{1}{\mu_{\text{int}}} \right)^{-1/3}, \quad (2)$$

where we have assumed $k = 1/\mu_{\text{app}} - 1/\mu_{\text{int}}$ as in our previous Preisach analysis.

III. DISCUSSION

Figure 3 shows the behavior of the correlation length δ_c estimated from the dynamic Preisach analysis and Barkhausen experiments. For both samples A and B, Barkhausen-effect data are in good agreement with Eq. (2) at low permeabilities. A definite deviation is observed in sample A at high μ_{app} , where the value $\delta_c \cong 25 \mu\text{m}$ is approached. This value is only slightly smaller than the Preisach correlation length. It is worth noting that some differences should be expected as the Barkhausen estimation represents the zero-frequency extrapolation of the results obtained at low-magnetization frequencies, while the Preisach length is obtained in the dynamic case. Interestingly, both the Barkhausen and the Preisach correlation lengths are close to the grain size, a result confirming that a single structural length governs all aspects of the magnetization process when the grain size is lower than the ribbon thickness.

The role of the ribbon thickness becomes more evident in sample B ($\langle s \rangle = 160 \mu\text{m}$). The Barkhausen correlation length does not show any clear approach to a constant value. Due to experimental difficulties, measurements could not be performed at permeabilities close to μ_{int} , so we cannot test if δ_c would eventually become similar to that of sample A. The Barkhausen correlation region is approximately half of the Preisach correlation length, with the latter close to the ribbon thickness. Contrary to sample A, this result points at the ribbon thickness as the characteristic length playing the main role in the dynamic magnetization process.

We can conclude that both ribbon thickness and typical grain size compete in determining the magnetization reversal features. Further experiments with different grain size/thickness ratios are required, especially at very small grain size to confirm the precise influence of the microstructure on the static and dynamic hysteresis of soft-magnetic materials.

ACKNOWLEDGMENT

The authors wish to thank Enzo Ferrara for providing the samples.

¹M. Shiozaki and Y. Kurosaki, J. Mater. Eng. **11**, 37 (1989).

²C. Appino, G. Durin, V. Basso, C. Beatrice, M. Pasquale, and G. Bertotti, J. Phys. IV **8**, 531 (1998).

³C. Appino, G. Durin, V. Basso, C. Beatrice, M. Pasquale, and G. Bertotti, J. Appl. Phys. **85**, 4412 (1999).

⁴P. Cizeau, S. Zapperi, G. Durin, and H. E. Stanley, Phys. Rev. Lett. **79**, 4669 (1997); S. Zapperi, P. Cizeau, G. Durin, and H. E. Stanley, Phys. Rev. B **58**, 6353 (1998).

⁵G. Durin and S. Zapperi, J. Appl. Phys. **87**, these proceedings (2000); Phys. Rev. Lett. (submitted).

⁶V. Basso, G. Bertotti, A. Infortuna, and M. Pasquale, IEEE Trans. Magn. **31**, 4000 (1995).

⁷G. Bertotti, IEEE Trans. Magn. **28**, 2599 (1992).

⁸G. Durin, A. Magni, and G. Bertotti, Fractals **3**, 351 (1995).

⁹I. D. Mayergoyz, *Mathematical Model of Hysteresis* (Springer, Berlin, 1991).

¹⁰J. S. Urbach, R. C. Madison, and J. T. Markert, Phys. Rev. Lett. **75**, 276 (1995); D. Spasojevic, S. Bukvic, S. Milosevic, and H. E. Stanley, Phys. Rev. E **77**, 2531 (1996); M. Bahiana *et al.*, *ibid.* **59**, 3884 (1999).